White Rose Research Online

eprints@whiterose.ac.uk
https://eprints.whiterose.ac.uk
Universities of Leeds, Sheffield and York

Deposited via The University of Sheffield.

White Rose Research Online URL for this paper:
https://eprints.whiterose.ac.uk/id/eprint/86803/

Version: Accepted Version

Article:
Li, G.J. and Zhu, Z.Q. (2015) Analytical modelling of modular and unequal tooth width surface-mounted permanent magnet machines. IEEE Transactions on Magnetics. ISSN: 0018-9464

https://doi.org/10.1109/TMAG.2015.2432735

© 2015 IEEE. Personal use of this material is permitted. Permission from IEEE must be obtained for all other users, including reprinting/ republishing this material for advertising or promotional purposes, creating new collective works for resale or redistribution to servers or lists, or reuse of any copyrighted components of this work in other works.

Reuse
Items deposited in White Rose Research Online are protected by copyright, with all rights reserved unless indicated otherwise. They may be downloaded and/or printed for private study, or other acts as permitted by national copyright laws. The publisher or other rights holders may allow further reproduction and re-use of the full text version. This is indicated by the licence information on the White Rose Research Online record for the item.

Takedown
If you consider content in White Rose Research Online to be in breach of UK law, please notify us by emailing eprints@whiterose.ac.uk including the URL of the record and the reason for the withdrawal request.

UNIVERSITY OF LEEDS
University of Sheffield
UNIVERSITY of York

Analytical Modelling of Modular and Unequal Tooth Width Surface-mounted Permanent Magnet Machines

G. J. Li, *Member*, *IEEE*, and Z. Q. Zhu, *Fellow*, *IEEE*

***Abstract* — This paper presents simple analytical modelling for 2 types of 3-phase surface-mounted permanent magnet (SPM) machines such as modular and unequal tooth width (UNET) machines with different slot/pole number combinations. It is based on the slotless open-circuit air-gap flux density and the slotted air-gap relative permeance calculations. This model allows calculating the open-circuit air-gap flux density, phase flux linkage and back electromotive force (EMF), average torque of both the modular and UNET machines. Its accuracy has been validated by 2D finite element (FE) method. A flux focusing/defocusing factor has also been introduced to analyse the influence of flux gaps in alternate stator teeth of modular machines on the machine electromagnetic performances. It has been found that by properly choosing the slot/pole number combination and flux gap width, the open-circuit air-gap flux density, the winding factor and the flux focusing effect can all be improved. As a result, the performance of modular machine can be significantly boosted. The analytical and FE models have been validated by experiments.**

***Index Terms* — Analytical modelling, finite element, modular, permanent magnet, unequal tooth.**

I. Introduction

PERMANENT magnet (PM) machines are attracting increasing interest due to their high torque density and high efficiency. They are widely used in domestic appliances, low CO_2 emission transports and renewable energy, etc. For example, large PM machines are being used for wind power generators. To simplify their manufacturing and transportation, modular structures, particularly modular stators, are widely adopted. The modular structures also inherently exhibit advantages such as higher fault tolerant capability and easier maintenance compared to their non-modular counterparts, making them well suitable for safety critical applications such as more electrical air-craft and aerospace.

The influence of modular stator such as individual stator tooth/back-iron segments or separate stator tooth segments and back-iron segments on electromagnetic performances has been investigated in [1]. It is found that the non-uniform additional air-gap between segments has increased the cogging torque by ≈ 4 times while reduced the EMF and hence average torque by ≈ 27%. However, a new modular structure by removing the PM in alternate stator teeth of a conventional linear switched flux permanent magnet (SFPM) machine has been proposed in [2]. Using the same amount of PM, the newly proposed modular machines can produce higher torque density. Similarly, [3]-[6] have proposed modular flux concentrating machine with modular stator and also modular rotor, the active mass of which is lower while the efficiency is slightly higher when compared to their non-modular counterparts.

By inserting flux gaps into alternate stator teeth, a new modular surface mounted permanent magnet (SPM) machine with segmented stator [see Fig. 1 (a) and (c), machine parameters are given in TABLE I] has been first introduced in [7] and been comprehensively investigated in [8] and [9] by using 2D FE modelling. Different slot/pole combinations have been compared and a general rule has been established: for machines with slot number (N_s) higher than pole number ($2p$, p is pole pair number), the flux gaps deteriorated the machine performances such as reducing the average torque. However, for machines with N_s lower than $2p$, the flux gaps can boost the machine performance by increasing average torque. This means that the modular structure can exhibit previously mentioned merits such as simple manufacturing and also better electromagnetic performance. However, the influence of flux gaps on open-circuit air-gap flux density and the flux focusing or defocusing effect due to flux gaps has not been quantified due to lack of in-depth understanding of the mechanism of modular machines. To fill this gap, a flux focusing or defocusing factor will be introduced and a simple analytical modelling based on slotless open-circuit flux density [10] and slotted air-gap relative permeance [11]-[12] will be carried out, which can provide a powerful insight into the real nature of novel modular machines. The contribution of this paper is therefore to propose a design guideline using simple analytical modelling for the future design practice of all non-modular, UNET and modular SPM machines with different slot/pole number combinations. For the purpose of comparison with modular machines, the unequal tooth width (UNET) SPM machines [see Fig. 1 (b) and (d)] will also be studied, which does not have flux focusing or defocusing effect and mainly influence the open-circuit flux density and the winding factor as investigated in [13]-[16].

This paper is organized as follows: the features of modular and UNET machines are briefly introduced in section II. The slotted open-circuit air-gap flux density, phase back-EMF and on-load average torque are calculated analytically and compared with their relevant 2D FE counterparts in section III. The analytically and FE predicted back-EMF waveforms are compared with the measured result in section IV. Conclusions are given in section V.

II. Features of Modular and UNET Machines

The topologies of modular and UNET machines used for analytical modelling in this paper are similar to that been investigated in [7] and [9], as shown in Fig. 1. Fig. 1 (a) and (c) show modular machines without/with tooth tips while with flux gaps in alternate stator teeth. The flux gap width (β_0 in degree) can be varied according the specifications. However, the iron section width (t_0) is kept constant in order to maintain the same magnetic saturation in stator iron core. The single layer windings are employed, which are wound on the stator teeth

without flux gaps. For the comparison purpose, the UNET stator can be achieved simply by filling in the flux gaps of modular stator with the same iron material as stator iron core, as shown in Fig. 1 (b) and (d). Only 10-pole rotors have been used in Fig. 1. However, other rotor pole numbers can also be employed, so the performance of modular and UNET machines with different slot/pole number combinations can be investigated.

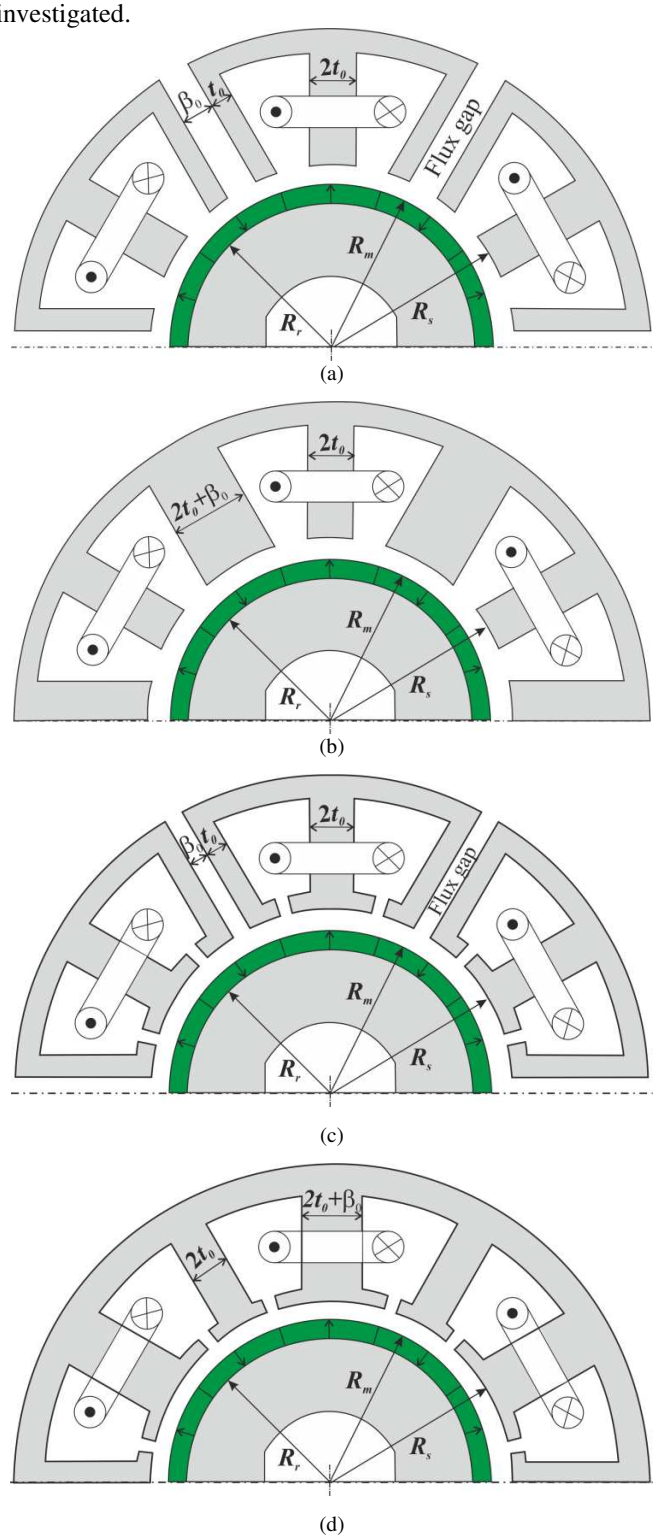

Fig. 1 Cross-sections of modular and UNET machines either with or without tooth tips. By way of example, the slot number is 12 while pole number is 10. (a) and (b) are modular and UNET machines without tooth tips, (c) and (d) are modular and UNET machines with tooth tips.

The main dimensions such as the stator inner radius (R_s), the rotor core and PM outer radii (R_r and R_m) will be used for analytical modelling. Other key parameters of the investigated machines are given in TABLE I.

TABLE I MOTOR PARAMETERS

Rated current (A_{RMS})	7.34	Stator tooth body width (mm)	7.1
Rated speed (rpm)	400	Stack length (mm)	50
Slot number	12	Air-gap length (mm)	1
Pole number	10/14	Rotor outer radius (mm)	27.5
Stator outer radius (mm)	50	Magnet thickness (mm)	3
Stator inner radius (mm)	28.5	Magnet remanence (T)	1.2
Stator yoke height (mm)	3.7	Number of turns per phase	132

III. Analytical Modelling of Modular and UNET SPM Machines

To investigate the machine performance using analytical modelling, the slotted open-circuit air-gap flux density should be calculated first. Then, integrating the open-circuit air-gap flux density from one coil pitch can give the coil flux linkage and hence the phase back-EMF by introducing the winding factor. Finally, the average torque can be calculated based on the obtained phase back-EMF and the given phase current.

In order to simplify the analytical calculation of air-gap flux density, the following assumptions should be made [11]-[12]:

- The permeability of iron core is infinite, no magnetic saturation is considered;
- Only the radial open-circuit air-gap flux density has been taken into account, the tangential component will not be considered;
- The tooth tip height is large enough so that the tooth body can be regarded as enlarged to be equal to the tooth tip width. As a result, the modelling of modular machine shown in Fig. 1 (c) will be similar to that in Fig. 1 (a), and the modelling of UNET machine shown in Fig. 1 (d) will be similar to that in Fig. 1 (b);
- 2-D problems, end-effects are neglected.

A. Open Circuit Air-Gap Flux Density

a. Air-Gap Relative Permeance

In the two-dimensional (2D) polar coordinate system, the air-gap flux density distribution due to PM in a slotless PM machines with surface-mounted parallel-magnetized PM can be calculated by [10]-[11]

$$B_{PM}(r,\alpha,\theta) = \sum_{n=1,3,5\ldots}^{\infty} K_B(n) f_{Br}(r) \cos[np(\alpha-\theta)] \quad (1)$$

where r is the radius in air-gap, α is angular position in air-gap, θ is rotor position, and n is harmonic order, respectively. $K_B(n)$ and $f_{Br}(r)$ are factors that depend on the machine parameters such as the number of pole pairs p, the rotor and magnet outer radii, the stator inner radius, the magnet remanence and the magnet arc to pole pitch ratio, as described in Appendix.

Then, the air-gap flux density of slotted SPM machine can be calculated by introducing the slotted air-gap relative permeance $\lambda_{rel}(\alpha)$, such as

$$B_{airgap}(r,\alpha,\theta) = B_{PM}(r,\alpha,\theta)\lambda_{rel}(\alpha) \quad (2)$$

with

$$\lambda_{rel}(\alpha) = \frac{\lambda}{[\mu_0/(g + h_m/\mu_r)]} \tag{3}$$

where μ_0 is the permeability of free space, g is the air-gap length, h_m is the magnet thickness, and μ_r is the recoil permeability of magnets, respectively.

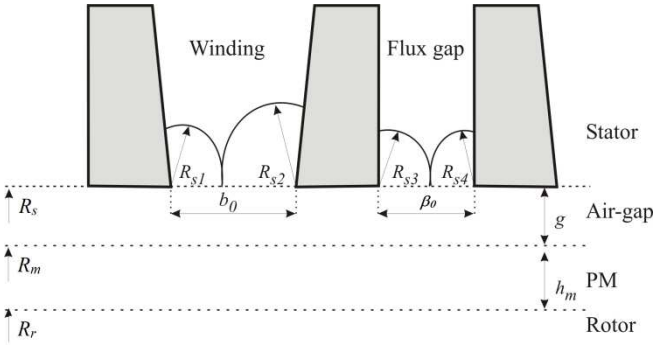

Fig. 2 Idealised flux paths in slot opening as well as in flux gap. Where b_0 is the slot opening angle while β_0 is flux gap opening angle, both are in mec. deg. R_{s1}, R_{s2}, R_{s3} and R_{s4} are the flux path lengths in slot openings and flux gaps.

Since machines with or without tooth tips can be modelled similarly based on previous assumptions, for simplicity, only the modular and UNET machines without tooth tips [see Fig. 1 (a) and (b)] will be used for analytical modelling in this paper. For modular machines with flux gaps in the middle of alternate stator teeth, the two sides of flux gaps are parallel as can be seen in Fig. 2. As a result, the permeance of flux gaps can be calculated by [11]

$$\lambda = \frac{\mu_0}{\left(g + \frac{h_m}{\mu_r} + \frac{\pi R_s \alpha}{2}\right)} \tag{4}$$

for $(N-1)\tau_s < \alpha < (N-1)\tau_s + \frac{\beta_0}{2}$, and

$$\lambda = \frac{\mu_0}{\left[g + \frac{h_m}{\mu_r} + \frac{\pi R_s(\beta_0 - \alpha)}{2}\right]} \tag{5}$$

for $(N-1)\tau_s + \frac{\beta_0}{2} < \alpha < (N-1)\tau_s + \beta_0$, where N can change from 1 to N_S, and $\tau_s = 2\pi/N_s$ is the slot pitch (equal to coil pitch for investigated machines), respectively. However, as shown in Fig. 1 (a) and (b), the two sides of slot openings are not parallel, and hence the equations (4) and (5) cannot be utilized any more. In order to overcome this difficulty, based on the flux path pattern in slot openings, as shown in Fig. 2, another method has been proposed in [12] such as

$$\Gamma(\alpha) = \frac{\pi R_s}{2} \frac{\sin\left(\frac{\alpha}{2}\right)\sin\left(\frac{b_0}{2} - \frac{\alpha}{2}\right)}{\sin\left(\frac{b_0}{4}\right)\cos\left(\frac{\alpha}{2} - \frac{b_0}{4}\right)} \tag{6}$$

where $\Gamma(\alpha)$ is resultant length of flux paths in slot openings. In all machines (UNET and modular), the flux lines in slot openings are considered parallel as shown in Fig. 2. As a result, the permeance in stator slot openings can be calculated by

$$\lambda = \frac{\mu_0}{\left[g + \frac{h_m}{\mu_r} + \Gamma(\alpha)\right]} \tag{7}$$

By way of example, the relative air-gap permeances for machines have been analytically calculated using equations from (3) to (7), as shown in Fig. 3. For UNET machines, the unequal tooth width will only enlarge the constant relative air-gap permeance range facing alternate stator teeth, as shown in Fig. 3 (a). However, for modular machines, the flux gap openings, similar to slot openings, lead to extra reduction in relative permeance at angular positions such as multiples of 30 mech. deg., as shown in Fig. 3 (b).

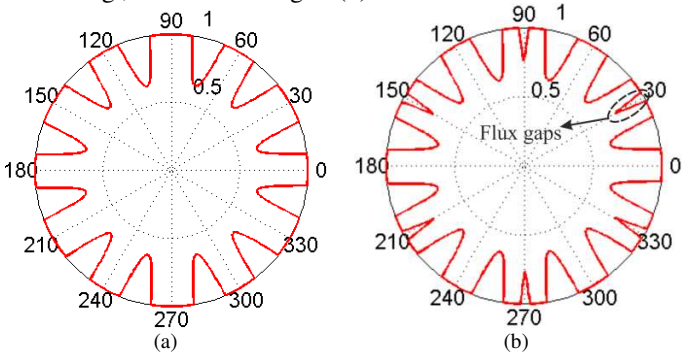

Fig. 3 Slotted air-gap relative permeance for 12-slot UNET and modular machines without tooth tips. $\beta_0 = 2$ mm. (a) UNET stator, (b) modular stator.

b. Open-Circuit Air-Gap Flux Density

Due to the previously mentioned influence of unequal tooth width and flux gaps on air-gap permeance, there will also be an impact on the air-gap flux density. This has been proven by the 2D FE open-circuit field distributions, as shown in Fig. 4, and detailed in [7]-[9]. It has been found that the flux gaps, having high reluctance, change dramatically the flux paths in stator iron core. As a result, the waveform of open-circuit air-gap flux density has been changed as well, as shown in Fig. 5.

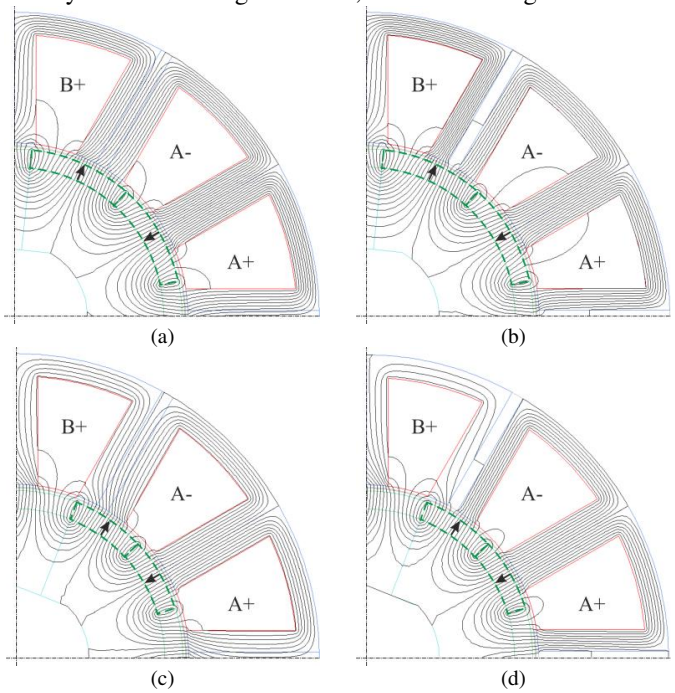

Fig. 4 Open-circuit flux line distributions of different 12-slot typed SPM machines, where the rotor position is for the phase A to have its maximum flux linkage. (a) UNET (12/10), (b) Modular (12/10), (c) UNET (12/14), (d) Modular (12/14).

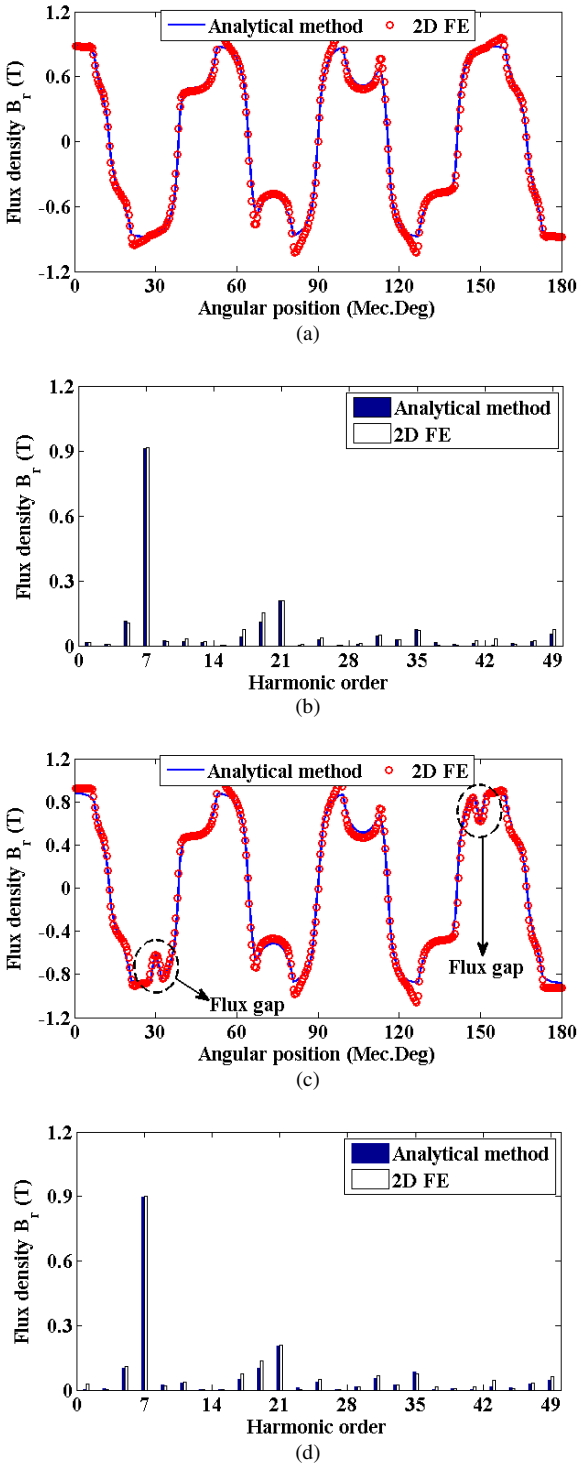

Fig. 5 Open-circuit air-gap flux density for 12-slot/14-pole modular and UNET machines with β_0 = 2 mm. (a) flux density (UNET), (b) spectra (UNET), (c) flux density (modular), (d) spectra (modular).

By way of example, the open-circuit air-gap flux densities of 12-slot/14-pole UNET and modular machines with β_0 = 2 and 4.5 mm has been calculated using equation (2) and compared with the relevant 2D FE results, as shown in Fig. 5 and Fig. 6, respectively. For a 12-slot/14-pole machine, the fundamental of air-gap flux density is 7th order harmonic, which contributes to torque generation. A good agreement has been observed for all the main harmonics such as 7th, 21st, 35th, etc. between the analytical and 2D FE results. As a result, the accuracy of analytical modelling can be validated.

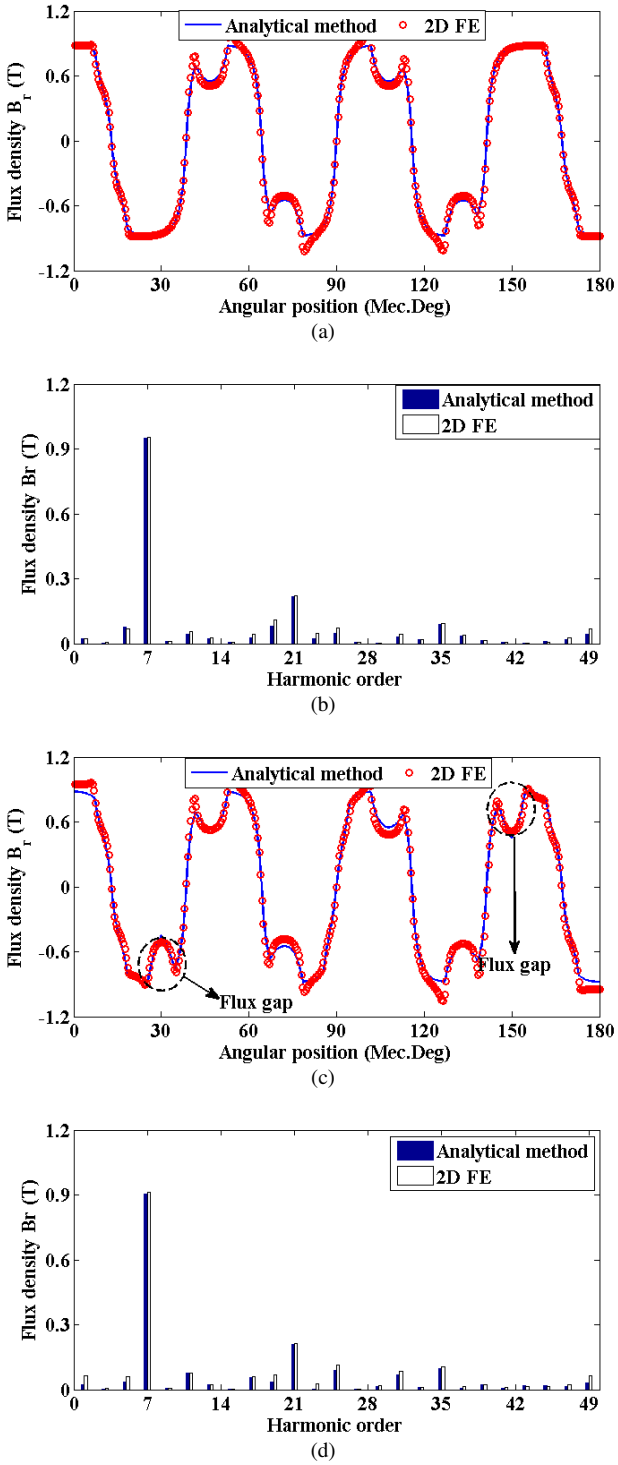

Fig. 6 Open-circuit air-gap flux density for 12-slot/14-pole modular and UNET machines with β_0 = 4.5 mm. (a) flux density (UNET), (b) spectra (UNET), (c) flux density (modular), (d) spectra (modular).

The harmonic contents in air-gap flux densities of 12-slot/10-pole and 14-pole UNET and modular SPM machines have also been calculated for different β_0. In Fig. 7, only the fundamentals are given because they largely determine the phase back-electromotive force (EMF) and hence output torque. It is found that the influence of unequal tooth width and

flux gap on air-gap flux density is nearly independent of the slot/pole number combinations. Besides, for UNET machines, the fundamental of air-gap flux density increases with the increase in β_0. This is mainly due to the reduction of slot opening, and hence reduction of effective air-gap length. However, the fundamental of air-gap flux density of modular machines first increases up to certain β_0, then begin to decline afterwards. This is mainly due to the fact that the increase in flux gap width will not necessarily lead to the increase in slot + flux gap opening because the slot opening is reducing. Meanwhile, as shown in Fig. 4, the flux gaps can reduce part of short-circuited fluxes due to stator tooth (flux gaps work as filter: increasing fundamental by reducing other harmonic contents [7]), and hence increase slightly flux density as proven by Fig. 7. This influence of unequal tooth width and flux gaps will partially be reflected in the phase back-EMF as detailed in section B.

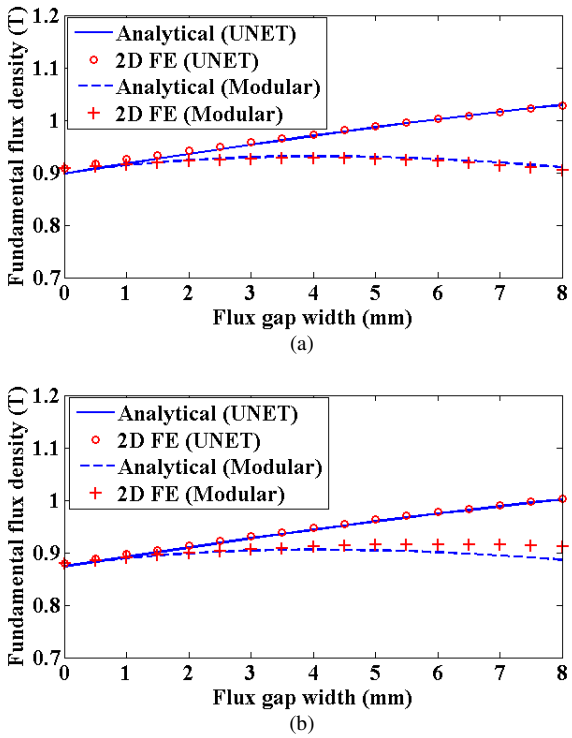

Fig. 7 Fundamental air-gap flux density vs flux gap width β_0 for UNET and modular SPM machines with different slot/pole number combinations. (a) 12-slot/10-pole, (b) 12-slot/14-pole.

B. Phase Back-EMF

The phase back-EMFs of conventional or unequal tooth width SPM machines are determined by the air-gap flux density and winding factor. However, for modular machines, due to the flux gaps in alternate stator teeth, a flux focusing or defocusing effect, depending on slot/pole number combinations, should be taken into account. Since the air-gap flux density has already been detailed previously, the following sections will focus on the winding factor and flux focusing/defocusing calculation.

In order to calculate the phase back-EMF, the distribution factor (k_{dn}), the coil pitch factor (k_{pn}) and hence the winding factor (k_{wn}) for different harmonics should be calculated first, the general expressions of which are described as follows:

$$k_{dn} = \frac{\sin(qn\sigma/2)}{q\sin(n\sigma/2)} \tag{8}$$

$$k_{pn} = \sin\left(n\frac{\tau_s}{\tau_p}\frac{\pi}{2}\right) = \sin\left(n\frac{p\pi}{N_s}\right) \tag{9}$$

$$k_{wn} = k_{pn} \times k_{dn} \text{ for } n = 1, 3, 5\ldots \tag{10}$$

where q is the number of coils per phase, σ is the phase angle between two adjacent coil vectors of one phase (in Elec. Deg).

In order to minimize the unbalanced magnetic force, even number of coils per phase is needed for modular and UNET machines. Therefore, the number of stator slots for 3-phase modular and UNET machines must be multiples of 12. As a result, the maximum distribution factor of 1 can always be achieved [8]-[9]. Moreover, it is also found that the variation of flux gap width or unequal tooth width has no effect on the distribution factor.

It should be noted that the pitch factor described by equation (9) is only for the machine with exactly the same stator tooth width. However, for UNET and modular machines as shown in Fig. 1, the coil pitches of which change with the variation of β_0. Thus, some modifications should be performed to take into account the influence of unequal tooth width or flux gap width (β_0) for calculating the pitch factors. Accordingly, the pitch factor becomes

$$k'_{pn} = \sin\left(\frac{n\pi}{2}\left(\frac{\tau_s - \beta_0}{\tau_p}\right)\right) \tag{11}$$

As mentioned previously, for calculating the phase EMF of modular machines, a flux focusing/defocusing factor (k_{fn}) needs to be introduced in order to account for the flux focusing or defocusing effect due to flux gaps. It has been found that the factor k_{fn} mainly depends on the slot/pole number combinations, and for different slot/pole number combinations, it can be described by

$$k_{fn}(N_s, 2p) = -\frac{(\beta_0/2)}{\tau_p} \tag{12}$$

for $N_s = 2p + 1$, $N_s = 2p + 2\ldots$ (slot number > pole number) such as 12-slot/10-pole.

$$k_{fn}(N_s, 2p) = \begin{cases} \dfrac{(\beta_0/2)}{\tau_p} & \text{for } \tau_s - \beta_0/2 \geq \tau_p \\ -\dfrac{(\beta_0/2)}{\tau_p} & \text{for } \tau_s - \beta_0/2 < \tau_p \end{cases} \tag{13}$$

for $N_s = 2p - 1$, $N_s = 2p - 2\ldots$ (slot number < pole number) such as 12-slot/14-pole. The calculation of factor k_{fn} can be explained by using the diagram shown in Fig. 8 and the real flux line distribution shown in Fig. 4 (c) and (d). For simplicity, only the case for machines with $N_s < 2p$ ($\tau_s > \tau_p$) has been analyzed. It can be seen from Fig. 4 and Fig. 8 that without flux gaps, the flux from a tube with a width of $\beta_0/2$ of North Pole PM (N) will enter into the stator segment #2. However, when flux gaps are introduced, the flux from the same PM tube will be forced to enter into the segment #1 because the flux path into segment #2 will experience longer effective air-gap (> $\beta_0/2$ + air-gap

length). The coil of segment #1 will have increased peak flux linkage and hence the flux gaps have flux focusing effect. Moreover, the quantity of increased flux will be $\frac{(\beta_0/2)}{\tau_p}$ of one full arc magnet (1 pole pitch) as given in (13). The negative sign on the right hand side of equation (13) means when flux gap width β_0 is too large, and the resultant coil pitch $\tau_s - \beta_0/2$ becomes smaller than pole pitch (similar to 12-slot/10-pole modular machine), the flux gaps will then have a flux defocusing effect. It is worth noting that for UNET machines, $k_{fn}(N_s, 2p) = 0$. Moreover, the factor k_{fn} will not be influenced by magnetic saturation and hence valid for both linear and no-linear conditions.

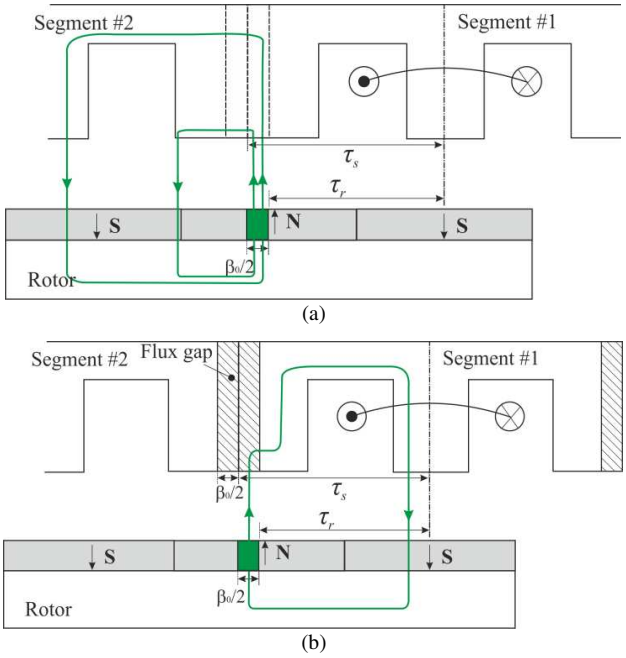

Fig. 8 Diagram showing the calculation of flux focusing or defocusing factor. In this figure, only the flux focusing effect has been shown. The real flux line distribution is shown in Fig. 4 (c) and (d). (a) flux line distribution without flux gaps (non-modular), (b) flux line distribution with flux gaps (modular).

Therefore, using the previous obtained open-circuit air-gap flux density and the factor k_{fn}, the flux linkage per coil can be calculated by

$$\Phi_{coil} = R_s N_c l_a (1 + k_{fn}) \sum_{n=1,3,5\ldots}^{\infty} \psi \cos(np\theta) \quad \text{with } \psi = \int_{-\left(\frac{\tau_s - \beta_0/2}{2}\right)}^{\left(\frac{\tau_s - \beta_0/2}{2}\right)} B_{airgap}(r, \alpha, \theta) d\alpha \tag{14}$$

where N_c is the number of turns per coil.

Derived from the previously obtained flux linkage, the phase back-EMF for the foregoing machines can be calculated by [13] and [17],

$$\text{EMF} = 2R_s N_p l_a \Omega (1 + k_{fn}) \times \sum_{n=1,3,5\ldots}^{\infty} k_{dn} f_{Br}(n) K_B(n) \sin(np\theta) \tag{15}$$

where N_p is number of turns per phase, Ω is the rotor mechanical speed, respectively.

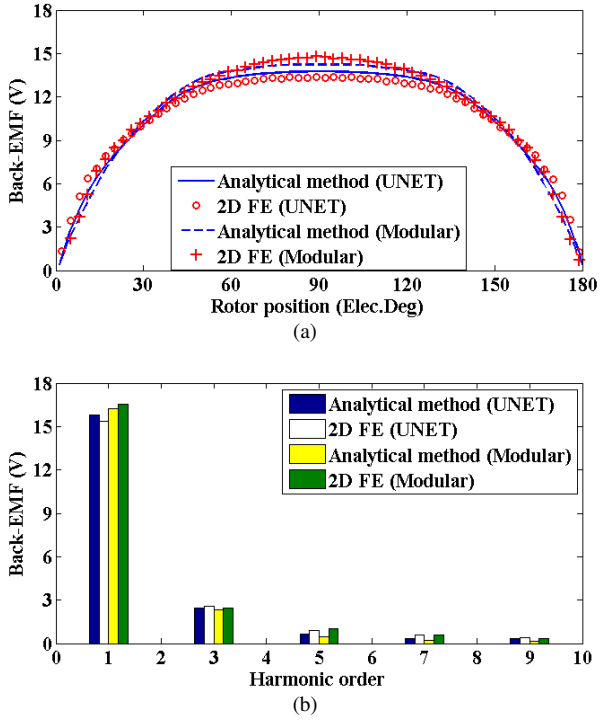

Fig. 9 Phase back-EMF for 12-slot/14-pole UNET and modular SPM machines with $\beta_0 = 2$ mm. (a) back-EMF, (b) spectra.

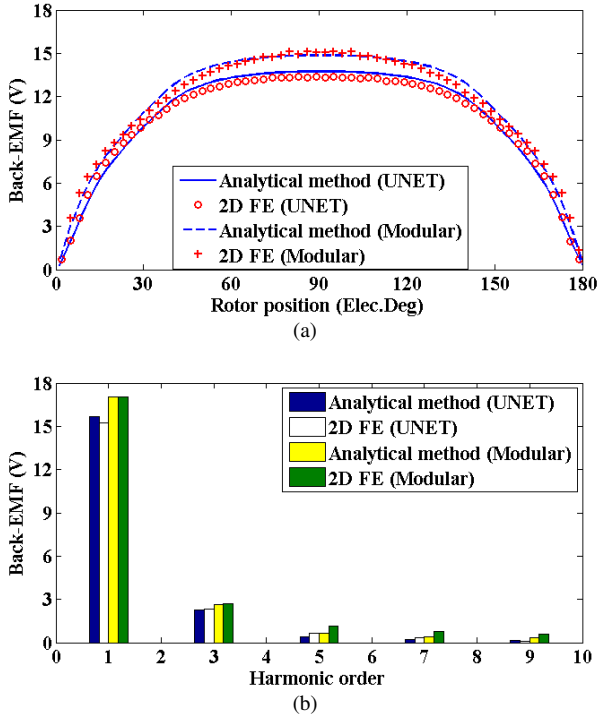

Fig. 10 Phase back-EMF for 12-slot/14-pole UNET and modular SPM machines with $\beta_0 = 4.5$ mm. (a) back-EMF, (b) spectra.

Using equations (12) - (15), the phase back-EMFs for UNET and modular machines have been calculated for different slot/pole number combinations and different β_0. By way of example, only the analytical results of 12-slot/14-pole UNET and modular machines with $\beta_0 = 2$ mm and $\beta_0 = 4.5$ mm are shown and compared with their relevant 2D FE

counterparts in Fig. 9 and Fig. 10, respectively. For consistency, the calculation of flux linkage using 2D FE is similar to equation (14) by directly integrating open-circuit air-gap flux density from $-\left(\frac{\tau_s-\beta_0/2}{2}\right)$ to $\left(\frac{\tau_s-\beta_0/2}{2}\right)$ for different rotor positions. The fundamentals obtained by analytical method and 2D FE match well. Nevertheless, there is difference for higher order harmonics, particularly the 5th and 7th, which mainly contribute to torque ripple under on-load conditions. Therefore, this mismatch will not affect the accuracy of average torque prediction as will be seen in section C.

The fundamentals of phase back-EMF against unequal tooth width and flux gap width for UNET and modular machines with different slot/pole combinations have also been calculated by analytical method. Since the average torque is proportional to back-EMF fundamental without accounting for the magnetic saturation, the relationship between back-EMF fundamental and β_0 is similar as that between average torque and β_0 as shown in Fig. 11, and will not be presented here to avoid duplication.

C. On-Load Electromagnetic Torque

Based on Park transformation and without accounting for flux weakening, the expression of average electromagnetic torque can be rewritten as

$$T_{average} = \frac{m}{2}\frac{E_1}{\Omega} I_q \tag{16}$$

where m is phase number (m = 3, in this paper), E_1 is the fundamental of phase back-EMF, and I_q is the q-axis current and equal to the amplitude of phase current, respectively.

Using equation (16), the average torques of UNET and modular machines have been analytically calculated for different β_0 and different slot/pole number combinations, and compared with the relevant 2D FE results, as shown in Fig. 11. It is found that except for the 12-slot/10-pole modular machine which has a maximum error of 6%, a good agreement between analytical and 2D FE average torques can be observed for all other machines and different β_0. It is also found that for 12-slot/10-pole machines, average torques reduce with the increase in β_0 regardless of UNET or modular structure. Nevertheless, the average torque of modular machine reduces quicker due to the extra flux defocusing effect from flux gaps. For both the 12-slot/14-pole UNET and modular machines, their average torques first increase to certain β_0 and begin to decline thereafter. This is mainly due to the fact that:

- For 12-slot/14-pole UNET machine, the average torque is determined by fundamental of open-circuit flux density [see Fig. 7 (b)] and the pitch factor [see (11), distribution factor is 1], giving the waveform of average torque against flux gap width as shown in Fig. 11 (b).
- However, for 12-slot/14-pole modular machine, the focusing/defocusing factor [see (13)] should be accounted for as well. When flux gap width is around 4.5 mm and $\tau_s - \beta_0/2 = \tau_p$, beyond which, the flux gaps will have a defocusing effect. This is why the average torque begins to decline.

It can be concluded that the developed simple analytical model can predict the performance such as air-gap flux density, phase back-EMF and on-load torque with acceptable accuracy. It is worth noting that the analytical model using simple air-gap relative permeance can also be extended to calculate the cogging torque by calculating the lateral force acting on the teeth [11]. This is however not the main scope of this paper, which is focused on the fast and accurate prediction of previously mentioned electromagnetic performance of all modular and UNET SPM machines with different slot/pole number combinations, flux gap widths, etc. In order to further improve the accuracy of predictions, the complex relative air-gap permeance [18], the conformal mapping [19], or subdomain analytical modelling [20], can be employed.

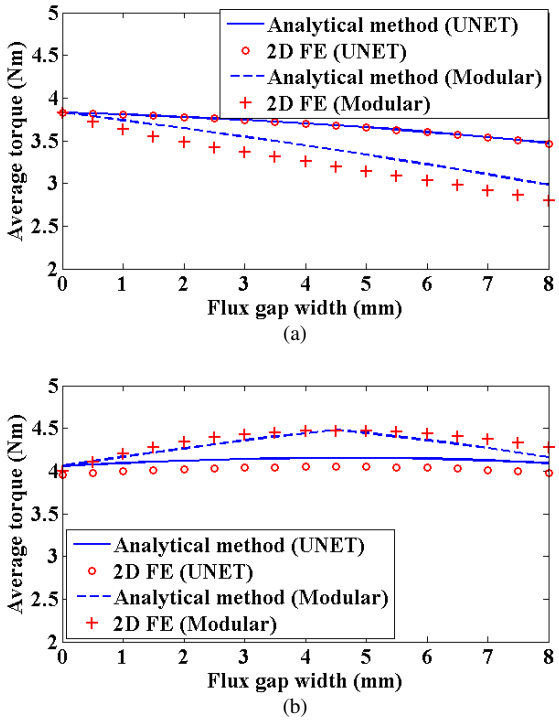

Fig. 11 Average torque vs β_0 for UNET and modular SPM machines with different slot/pole number combinations. (a) 12-slot/10-pole, (b) 12-slot/14-pole.

IV. Experimental Validation

A. Prototype modular machine

In order to validate the analytical and FE results, modular SPM machines have been built, as shown in the Fig. 12. The main dimensions of this modular machine are the same as in TABLE I while with a slot opening of 2 Mech. Deg.

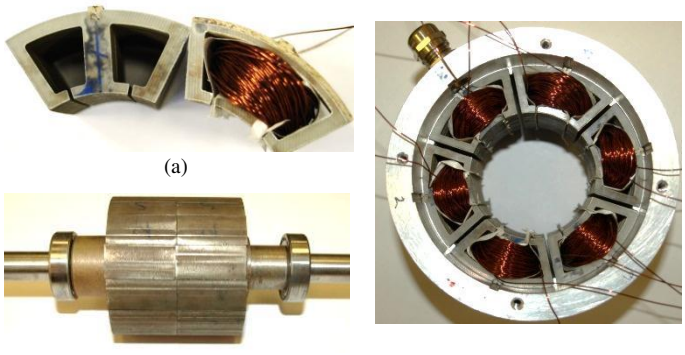

Fig. 12 Prototype machine with tooth tips. (a) unwound and wound stator segments, (b) 14-pole rotor, (c) completed stator and frame.

B. Phase back-EMF

The phase back-EMF at a rotor speed of 400 rpm has been calculated both analytically and numerically, and compared against measured results, as shown in Fig. 13. A good agreement can be observed and the slight difference is mainly due to the saturation effect that has not been accounted for in analytical models.

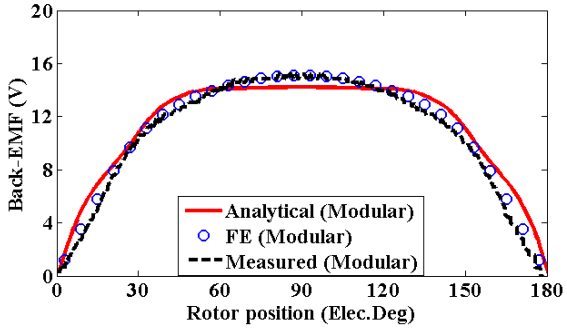

(a)

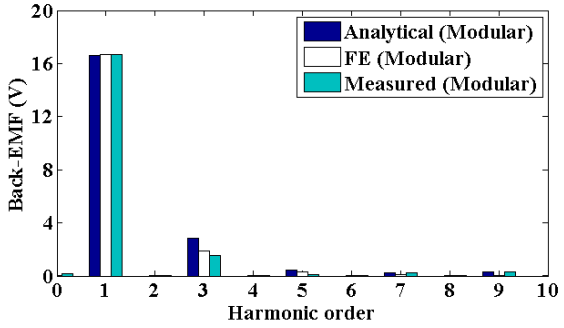

(b)

Fig. 13 Phase back-EMF for 12-slot/14-pole modular SPM machines with tooth tips and with β_0 = 2 mm. (a) back-EMF, (b) spectra.

V. Conclusion

A simple analytical method based on slotless air-gap flux density and slotted air-gap relative permeance has been developed to predict the open-circuit air-gap flux density, phase flux linkage and back-EMF, on-load average torque for unequal tooth width or modular SPM machines with different slot/pole number combinations and different flux gap widths as well as different unequal tooth widths. The accuracy of the analytical method has then been validated by 2D FE modelling and experiments.

It has been found that both the flux gaps and unequal teeth can improve the open-circuit air-gap flux density. However, the flux gaps, not only change the winding factor (more precisely, pitch factor) as unequal tooth width, but also introduce an extra flux focusing or defocusing effect (or factor) depending on the slot/pole number combination and the flux gap width itself. This makes the modular machines can either increase or reduce more the average torque compared to their unequal tooth width counter parts. Due to its simplicity, the analytical method and findings in this paper can be employed to cover other unequal tooth width and modular machines with different slot/pole number combinations, or with different phase numbers.

Appendix

As described in [10], for $np \neq 1$,

$$M_n = \frac{B_r}{\mu_0}\alpha_p[(A_{1n} + A_{2n}) + np(A_{1n} - A_{2n})] \tag{17}$$

where B_r is the magnet remanence, α_p is the magnet arc to pole pitch ratio, respectively.

With

$$A_{1n} = \frac{\sin[(np+1)\alpha_p\,\pi/(2p)]}{(np+1)\alpha_p\,\pi/(2p)} \tag{18}$$

And

$$A_{2n} = \frac{\sin[(np-1)\alpha_p\,\pi/(2p)]}{(np-1)\alpha_p\,\pi/(2p)} \tag{19}$$

While

$$A_{3n} = \left(np - \frac{1}{np}\right)\frac{M_{rn}}{M_n} + \frac{1}{np} \tag{20}$$

With

$$M_{rn} = \frac{B_r}{\mu_0}\alpha_p(A_{1n} + A_{2n}) \tag{21}$$

For internal rotor machines (see Fig. 1 and Fig. 2), in which stator inner radius (R_s) > PM outer radius (R_m) > rotor core outer radius (R_r), the $f_{Br}(n)$ can be written by

$$f_{Br}(n) = \left(\frac{r}{R_s}\right)^{np-1}\left(\frac{R_m}{R_s}\right)^{np+1} + \left(\frac{R_m}{r}\right)^{np+1} \tag{22}$$

And $K_B(n)$ can be written using equation (23).

$$K_B(n) = \frac{\mu_0 M_n}{2\mu_r}\frac{np}{(np)^2-1}\left\{\frac{(A_{3n}-1) + 2\left(\frac{R_r}{R_m}\right)^{np+1} - (A_{3n}+1)\left(\frac{R_r}{R_m}\right)^{2np}}{\frac{\mu_r+1}{\mu_r}\left[1-\left(\frac{R_r}{R_s}\right)^{2np}\right] - \frac{\mu_r-1}{\mu_r}\left[\left(\frac{R_m}{R_s}\right)^{2np} - \left(\frac{R_r}{R_m}\right)^{2np}\right]}\right\} \tag{23}$$

References

[1] Z. Q. Zhu, Z. Azar, and G. Ombach, "Influence of additional air gaps between stator segments on cogging torque of permanent-magnet machines having modular stators," *IEEE Trans. Mag.*, vol. 48, no. 6, pp. 2049-2055, Jun. 2012.

[2] M. J. Jin, C. F. Wang, J. X. Shen, and B. Xia, "A modular permanent-magnet flux-switching linear machine with fault-tolerant capability," *IEEE Trans. Mag.*, vol. 45, no. 8, pp. 3179-3186, Aug. 2009.

[3] E. Spooner, and C. Williamson, "Electromagnetic machine with at least one pair concentric rings having modulized magnets and yokes," US patent 5844341, Dec. 1, 1998.

[4] E. Spooner, and A. Williamson, "Modular, permanent-magnet

wind-turbine generators," in *Conf. Record of the 1996 IEEE Ind. Appl. Conf.*, 6-10 Oct. 1996, pp. 497-502.

[5] E. Spooner, A. C. Williamson, and G. Catto, "Modular design of permanent-magnet generators for wind turbines," *IEE Proc. Elec. Power Appl.*, vol. 143, no. 5, pp. 388-395, Sep. 1996.

[6] Z. Chen, and E. Spooner, "A modular, permanent-magnet generator for variable speed wind turbines," in *7th Int. Conf. (Conf. Publ. No. 412) Electrical Machines and Drives*, 11-13 Sep. 1995, pp. 453-457.

[7] G. Dajaku and D. Gerling, "Low costs and high-efficiency electric machines," in *2nd Int. Electric Drives Production Conf. (EDPC)*, 15-18 Oct. 2012, pp. 1-7.

[8] G. J. Li, Z. Q. Zhu, W. Q. Chu, M. P. Foster, and D. A. Stone, "Influence of flux gaps on electromagnetic performance of novel modular pm machines," *IEEE Trans. Energy Convers.*, vol. 29, no. 3, pp. 716-726, Sept. 2014.

[9] G. J. Li, Z. Q. Zhu, M. P. Foster, and D. A. Stone, "Comparative studies of modular and unequal tooth pm machines either with or without tooth tips," *IEEE Trans. Mag.*, vol. 50, no. 7, pp. 1-10, Jul. 2014.

[10] Z. Q. Zhu, D. Howe, and C. C. Chan, "Improved analytical model for predicting the magnetic field distribution in brushless permanent-magnet machines," *IEEE Trans. Mag.*, vol. 38, no. 1, pp. 229-238, Jan. 2002.

[11] Z. Q. Zhu, and D. Howe, "Analytical prediction of the cogging torque in radial-field permanent magnet brushless motors," *IEEE Trans. Mag.*, vol. 28, no. 2, pp. 1371-1374, Mar. 1992.

[12] B. Gaussens, E. Hoang, O. de la Barriere, J. Saint-Michel, M. Lecrivain and M. Gabsi, "Analytical approach for air-gap modeling of field-excited flux-switching machine: no-load operation," *IEEE Trans. Mag.*, vol. 48, no. 9, pp. 2505-2517, Sept. 2012.

[13] D. Ishak, Z. Q. Zhu, and D. Howe, "Permanent-magnet brushless machines with unequal tooth widths and similar slot and pole numbers," *IEEE Trans. Ind. Appl.*, vol. 41, no. 2, pp. 584- 590, Mar.-Apr. 2005.

[14] S. P. Cheng and C. C. Hwang, "Design of high-performance spindle motors with single-layer concentrated windings and unequal tooth widths," *IEEE Trans. Mag.*, vol. 43, no. 2, pp. 802-804, Feb. 2007.

[15] J. K. Xia, T. Dong, C. Y. Wang, and J. Y. Zhao, "Low speed high torque PMSM design based on unequal teeth structure," in *Int. Conf. Elec. Machines and Systems*, 17-20 Oct. 2008, pp. 3274-3277.

[16] S. Senol, and O. Ustun, "Design, analysis and implementation of a subfractional slot concentrated winding BLDCM with unequal tooth widths," in *37th Annual Conf. IEEE Ind. Electron. Soc.*, 7-10 Nov. 2011, pp. 1807-1812.

[17] D. Ishak, Z. Q. Zhu, and D. Howe, "Comparison of PM brushless motors, having either all teeth or alternate teeth wound," *IEEE Trans. Energy Convers.*, vol. 21, no. 1, pp. 95- 103, Mar. 2006.

[18] D. Zarko, D. Ban, and T.A. Lipo, "Analytical calculation of magnetic field distribution in the slotted air gap of a surface permanent-magnet motor using complex relative air-gap permeance," *IEEE Trans. Magn.*, vol. 42, no. 7, pp. 1828-1837, Jul. 2006.

[19] D. Zarko, D. Ban, and T. A. Lipo, "Analytical solution for cogging torque in surface permanent-magnet motors using conformal mapping," *IEEE Trans. Magn.*, vol. 44, no. 1, pp. 52–65, Jan. 2008.

[20] L. J. Wu, Z. Q. Zhu, D. A. Staton, M. Popescu, and D. Hawkins, "Comparison of analytical models of cogging torque in surface-mounted PM machines," *IEEE Trans. Ind. Electron.*, vol. 59, no. 6, pp. 2414-2425, June 2012.

G. J. Li (M'10) received his BEng, MSc and PhD degrees in electrical and electronic engineering from the Wuhan University, China, in 2007, University of Paris XI, France, in 2008, and the Ecole Normale Supérieure (ENS) de Cachan, Paris, France, in 2011, respectively. He joined the University of Sheffield in June 2012 as a post-doctoral research associate at EMD Group. Since September 2013, he took up a Lectureship in Electrical Engineering within the EMD Group at the University of Sheffield. His main research interests include the design, fault analysis and thermal management of electrical machines for renewable energy, automotive, more electrical aircraft, etc.

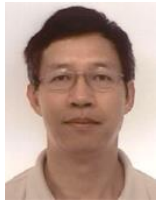

Z. Q. Zhu (M'90–SM'00–F'09) received the B.Eng. and M.Sc. degrees in electrical and electronic engineering from Zhejiang University, Hangzhou, China, in 1982 and 1984, respectively, and the Ph.D. degree in electrical and electronic engineering from the University of Sheffield, Sheffield, U.K., in 1991. Since 1988, he has been with the University of Sheffield, where he is currently a Professor of electrical machines and control systems, the Head of the Electrical Machines and Drives Research Group, and the Academic Director of the Sheffield Siemens Wind Power Research Centre. His current major research interests include the design and control of permanent-magnet brushless machines and drives for applications ranging from automotive to renewable energy.